Journal of Physics B: Atomic, Molecular and Optical Physics

PAPER

Direct frequency-comb spectroscopy of $6s^2S_{1/2}$–$8s^2S_{1/2}$ transitions of atomic cesium

To cite this article: Kyung-tae Kim and Jaewook Ahn 2018 *J. Phys. B: At. Mol. Opt. Phys.* **51** 035001

IOP Publishing Journal of Physics B: Atomic, Molecular and Optical Physics
J. Phys. B: At. Mol. Opt. Phys. **51** (2018) 035001 (4pp) https://doi.org/10.1088/1361-6455/aaa05e

Direct frequency-comb spectroscopy of $6s^2S_{1/2}$–$8s^2S_{1/2}$ transitions of atomic cesium

Kyung-tae Kim and Jaewook Ahn[1]

Department of Physics, KAIST, Daejeon 34141, Republic of Korea

E-mail: jwahn@kaist.ac.kr

Received 13 October 2017, revised 27 November 2017
Accepted for publication 8 December 2017
Published 8 January 2018

Abstract

Direct frequency-comb spectroscopy is used to probe the absolute frequencies of the $6s2S_{1/2}$–$8s2S_{1/2}$ two-photon transitions of atomic cesium in a hot vapor environment. By utilizing the coherent control method of temporally splitting the laser spectrum above and below the two-photon resonance frequency, Doppler-free absorption is built in two spatially distinct locations and imaged for high-precision spectroscopy. Theoretical analysis finds that these transition lines are measured with uncertainty below 5×10^{-10}, mainly contributed from laser-induced AC Stark shift.

Keywords: frequency-comb spectroscopy, two-photon transition, Stark shift

(Some figures may appear in colour only in the online journal)

1. Introduction

A frequency-comb laser generates a train of equally time-separated optical pulses and its spectrum is a comb of equally spaced frequency components, given by

$$f_n = f_{ceo} + nf_{rep}, \quad (1)$$

where f_{ceo} is the carrier-envelope offset frequency (often locked to a radio-frequency standard such as an atomic clock), f_{rep} is the comb tooth spacing (or the repetition frequency of a mode-locked laser), and n is an integer on the order of a million [1]. This laser provides absolute frequencies in an optical frequency domain that can be fine-tuned electronically. The linewidth of the comb modes can be quite narrow compared to transition linewidths, allowing for high-resolution spectroscopy, in spite of the large spectral range. The Doppler-free spectroscopy scheme using frequency combs was initially proposed for the 1s–2s transition of hydrogen [2] and later experimentally demonstrated [3]. This scheme has been widely used for various precision measurements in fundamental constants [4, 5], molecules and ions [6–8], and even distance-ranging applications [9].

Recently a coherent control method, which rather directly uses the frequency comb for spectroscopy than referencing continuous-wave (CW) lasers, was developed [10]. Termed as direct frequency-comb spectroscopy (DFCS), this method extends the usage of the frequency comb to Doppler-free spectroscopy of atoms in hot vapor environments. For example, rubidium 5s–7s transition lines were measured with enhanced accuracy [11]. This method is relatively simple to experimentally implement, compared to cold-atom based spectroscopy, and thus reduces systematic effects such as radiation pressure in cold-atom ensembles [12].

In this experiment, we probed the $6s^2S_{1/2}$ ($F = 3, 4$) $\rightarrow$ $8s^2S_{1/2}$ ($F' = 3, 4$) two-photon transitions of atomic cesium (^{133}Cs). As shown in figure 1(a), these transitions have excitation frequencies around 2×365 THz (822/2 nm in wavelength). As described below, we used the DFCS method adopted from [11] and the result is compared with the previous measurement performed with picosecond lasers frequency-stabilized to frequency-comb references [13].

2. Measurement principle and setup

The experimental setup for our DFCS is schematically illustrated in figure 1(b). We used a home-made Kerr-lens mode-locked Ti: sapphire laser-oscillator, which produced laser pulses frequency-centered at $f_L = 365$ THz ($\lambda_L = 822$ nm in wavelength) with a bandwidth of $\Delta f = 15$ THz (FWHM, $\Delta\lambda = 35$ nm). The pulse-repetition rate was controlled in the range from $f_{rep} = 80$ to 90 MHz and the carrier-envelope offset frequency from $f_{ceo} = 10$ to 30 MHz. Scanning the frequency within the comb spacing was performed through changing the reference frequency f_{rep}. We scanned f_{rep} by changing the cavity length

[1] Author to whom any correspondence should be addressed.

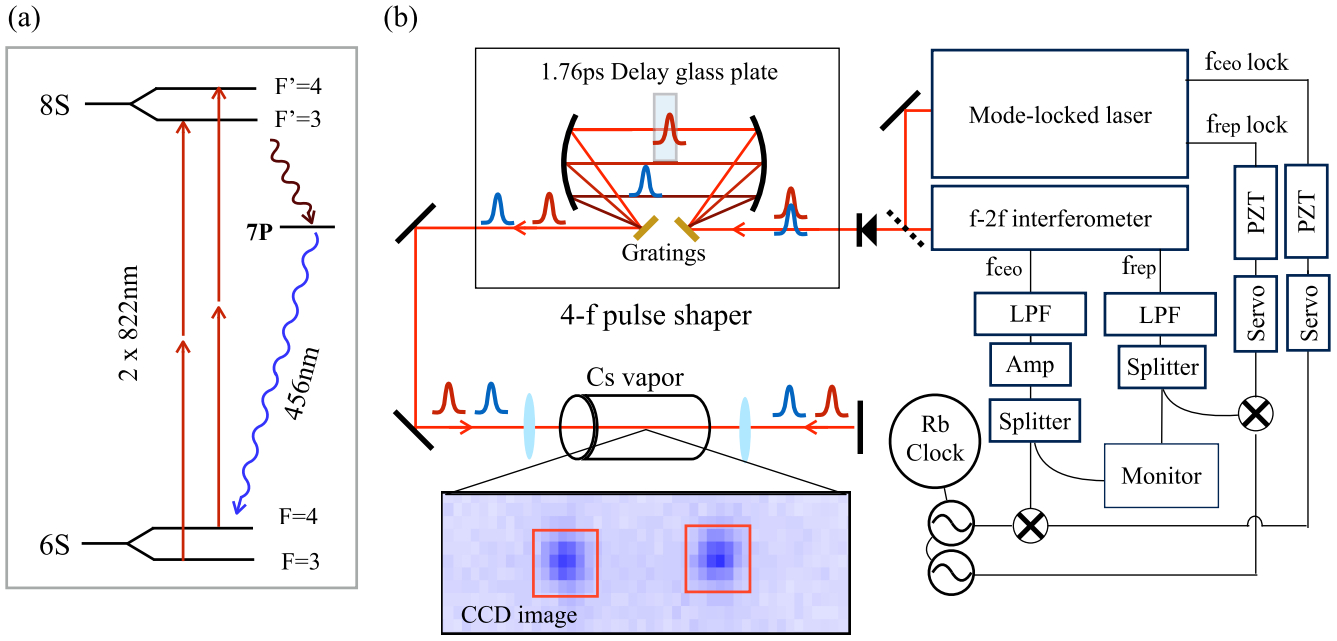

Figure 1. (a) Energy-level structure of atomic cesium (^{133}Cs). The two-photon transitions from $6s^2S_{1/2}$ ($F = 3, 4$) → $8s^2S_{1/2}$ ($F' = 3, 4$), having a two-photon resonance at around 822 nm. After the excitation, the 456 nm fluorescence from 7p was collected with a charge-coupled device (CCD) camera to record the population excited to the $8s^2S_{1/2}$ levels. (b) Experimental setup of DFCS. (PZT: piezoelectric inducer, LPF: low pass filter, Amp: amplifier).

using a PZT at the output coupler, while f_{ceo} was kept constant by adjusting the tilt of the end mirror. The spectral output of the comb was broadened using a photonic crystal fiber. We used a commercial supercontinuum generation module (FemtoWHITE 800 from NKT photonics), of which the fiber ends were sealed with quartz ferrules for ease of use and to reduce optical damage. The laser was then frequency stabilized with the conventional *f*-to-2*f* self-referencing Mach–Zehnder interferometer [14], where both f_{rep} and f_{ceo} were locked to a rubidium atomic clock using custom-made phase-locked feedback loops.

Single-sided Doppler-broadened two-photon absorption was avoided with a coherent control method [11]. The initial pulse spectrum was divided into two with respect to the exact two-photon center (the frequency that corresponded to half of the $6s^2S_{1/2}$–$8s^2S_{1/2}$ transition frequency). When we denote red (blue) pulse for the spectrum below (above) the two-photon center, the red and blue pulses should be applied to the atom at the same time, to satisfy the energy conservation of the two-photon transition. The red and blue pulses were separated in time and we created a replica of these two pulses that propagated in the opposite direction. Then, at two distinct positions, each red and blue pulse collided with its back-propagating counterpart (>94% of the forward laser intensity). In this case, because the directions of the red (blue) and its counterpart were opposite to each other, Doppler-free two-photon absorption (except residual shift due to the frequency difference between the red and blue) occurred at these two positions (see the CCD image in figure 1(b)).

However, because the lifetime of the excited state (≈1 μs) is longer than the typical pulse-repetition time (≈10 ns), the excited-state population can be coherently accumulated as the pulse train passes by. The amount of the accumulated population depends on the delay ($1/f_{rep}$) and the phase difference ($\propto f_{ceo}$) between subsequent pulse pairs. It can also be understood in the frequency domain: as the delay and the phase difference are the two comb parameters, f_{ceo} and f_{rep}, the situation becomes simply the summation of two-photon transition from the pairs of two CW lasers whose frequencies are determined by the comb parameters. This explanation is valid for the weak-field regime that corresponds to our experimental conditions.

In the setup shown in figure 1(b), each laser pulse was split to a pair of sub-pulses with a conventional *4f* geometry pulse shaper [15]. By placing a glass plate on the Fourier plane, the red spectrum pulse was time-delayed by 1.76 ps with respect to the blue part. No significant pulse broadening (less than 30fs FWHM) ensured that this plate gave no significant higher-order dispersion. We also controlled the laser power by cutting the laser spectrum with a knife edge on the Fourier plane. The red and blue sub-pulses counter-propagated and were focused with a beam waist of 50 μm, before they interacted with the atoms at the center of the vapor cell. Doppler-free $8s^2S_{1/2}$ excitation occurred at two distinct spatial locations. We measured the $8s^2S_{1/2}$ state population through a 8s → 7p → 6s decay channel, where the 456 nm fluorescence (7p → 6s) was imaged with a CCD. A typical image is shown in figure 1(b), and we integrated the red boxes at the image to extract a spectroscopy signal.

3. Result and discussion

Figure 2 shows a typical spectrum of the cesium $6s^2S_{1/2}$–$8s^2S_{1/2}$ transitions, where the left peak corresponds to $F = 3 \rightarrow F' = 3$ and the right $F = 4 \rightarrow F' = 4$. The

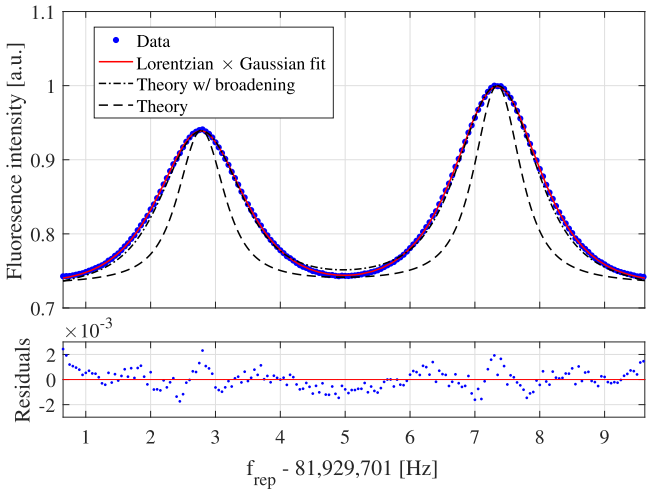

Figure 2. Doppler-free two-photon transition spectrum of ^{133}Cs $6s^2S_{1/2}$–$8s^2S_{1/2}$ transitions. The left peak corresponds to a $F = 3 \rightarrow F' = 3$ transition and the right to $F = 4 \rightarrow F' = 4$. Blue dots are experimental data points (integration of the spatial excitation pattern in figure 1) and the red line is its fit to the product of Lorentzian and Gaussian functions. For this measurement, we used 35 mW of laser power and 10 nm (FWHM) of spectral width and averaged 30 times. The *X*-axis can be converted to an optical frequency domain and 1 Hz in $\Delta f_{\rm rep}$ corresponds to 8.9 MHz in Δf [$f = 2f_{\rm ceo} + (m + n)f_{\rm rep}$, $\delta f = (m + n)\delta f_{\rm rep}$, $(m + n) \sim 8.9 \times 10^6$]. The linewidth is measured to be about 13 MHz (FWHM).

measured spectrum is compared with a theoretical absorption profile, which is a refined version from [11], given by

$$|a_f^{(2)}(f_{\rm rep})|^2 \approx \left\{ \sum_{m,n} \left(\frac{|E_m(f_{rep})E_n(f_{\rm rep})|^2}{(f_{\rm ceo} + nf_{\rm rep} - f_i)^2[(f_{\rm target} - 2f_{\rm ceo} - (m+n)f_{\rm rep})^2 + 1/4\tau_f^2]} \right) \circ G^D_{m,n}(f_{\rm rep}) \right\} \circ G^B(f_{\rm rep}), \quad (2)$$

where m and n are integers denoting the comb index, τ_f is the lifetime, and $\circ$ denotes convolution. $G^{\rm D}_{m,n}(f_{\rm rep}) = \exp\left[\left(\frac{c^2 m}{2k_{\rm B}T} \right) \left(\frac{f_i - 2f_{\rm ceo} - (m+n)f_{\rm rep}}{(m-n)f_{\rm rep}} \right)^2 \right]$ is the line-shape from the residual Doppler shift that comes from the imbalance between the momenta of two modes in each pair. $G^{\rm B}(f_{\rm rep})$ is the line-shape from the other broadening factors such as the laser linewidth (1.3 MHz) and transit-time broadening (1.6 MHz) in our experimental setup (in total, $G^{\rm B}(f_{\rm rep})$ is the Voigt profile). The theoretical model contains series of summations so that performing the fitting procedure is rather time consuming. So, the center frequency of the absorption line was extracted by fitting the data to the product of Lorentzian and Gaussian functions with its coefficients as free parameters. A typical fit and its residuals, along with the theoretical lines (including an offset), are shown in figure 2. The measured linewidth is an order of magnitude broader than the natural linewidth of this transition (~1 MHz), due to line broadening mechanisms, including the residual Doppler shift (~5 MHz), the laser linewidth (1.3 MHz over our integration time), and the transit-time broadening (1.6 MHz).

Table 1. Summary of the measured frequency of the $6s^2S_{1/2}$–$8s^2S_{1/2}$ transition of ^{133}Cs. All the frequencies are in MHz unit.

	$F = 3 \rightarrow F' = 3$	$F = 4 \rightarrow F' = 4$
This work	729, 014, 476.90(40)	729, 006, 160.73(33)
Fendel [13]	729, 014, 476.834(15)	729, 006, 160.702(15)
Stalnaker [16]	729, 014, 476.65(22)	729, 006, 160.58(22)

Our measurements are summarized in table 1, compared with previous measurements. Fendel *et al* in [13] used picosecond lasers frequency-stabilized to a frequency-comb laser and Stalnaker *et al* in [16] used self-reference frequency-comb lasers but each counter-propagating beam was color-filtered. Our measurement based on DFCS using coherent control method agrees well with these results, within the range of uncertainty.

Now we discuss the systematic errors caused by pressure shift, transient-time broadening, Zeeman shift, and AC Stark shift.

Pressure shift: previously measured pressure shifts are -26 kHz mTorr^{-1} (-12 kHz mTorr^{-1}) for $F = 4$ ($F = 3$) [17]. In our experimental conditions, the temperature of the vapor cell was maintained at around 60 °C and the corresponding vapor pressure was 3×10^{-5} Torr [21]. This leads to a pressure shift of -780 (-360) Hz for $F = 4$ ($F = 3$), which is smaller than our measurement resolution.

Transit-time broadening: the beam waist of our laser was around 50 μm, resulting in transit-time broadening [18] of $\delta f_{\rm t} = 0.4v/w = 1.6$ MHz, where $w = 50$ μm is the Gaussian beam waist and $v = 204$ m s^{-1} the most probable speed of atoms. Due to the small beam waist, the transit-time broadening was of a similar order in magnitude to the natural linewidth of 8s levels, but this does not shift the line centers.

Zeeman shift: Zeeman shifts of these transitions have been measured to be 2 kHz at 10 Gauss [13]. Our experimental region near the vapor cell was covered with μ-metal so there was negligible magnetic field. So, the Zeeman shift was within our measurement uncertainty.

AC Stark shift: AC Stark shifts in these transitions are known to be linearly proportional to the average laser intensity (not the laser peak intensity). According to [13], the AC Stark shift is around -0.21 Hz mW^{-1} cm^{-2}. In our experiment, the maximum intensity was around ~50 mW for a beam size around 50 μm. So, the expected shift of the line center is around -132 kHz at 50 mW laser power. This is the main, and only considerable, cause of the systematic error to the frequency shift, among the four considered above. Figure 3 shows the Stark shifts measured for various laser intensities (controlled by the pulse shaper). The unshifted frequency was obtained through extrapolating to zero field to estimate the slopes for the $F = 4$ and $F = 3$ transitions around $-7.4(0.9)$ kHz mW^{-1} and $-8.3(2.0)$ kHz mW^{-1}, respectively. We take the shift at typical experimental conditions, 34.8 mW, as the systematic error from AC Stark shift of our measurements, which give 289 kHz for $F = 4$ and 358 kHz for $F = 3$.

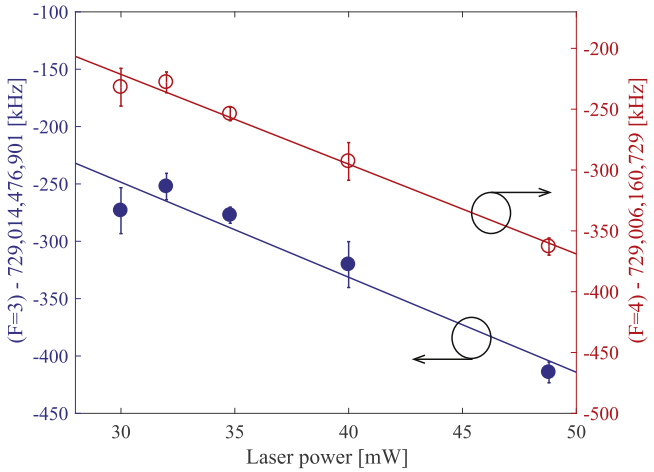

Figure 3. Dependence of the measured center frequency on the laser power. Void (filled) circles corresponds to $F = 4$ ($F = 3$) transition frequency. We extrapolate the transition frequencies to zero laser power. The error bar shows a standard error for each fitting.

The observed Stark shift is proportional to the average power instead of the peak power that might lead to much larger frequency shift. In the context of the time-domain population dynamics [19], the excited-state population is determined by the phase difference of the sequential excitation probability amplitudes given by the train of pulses, and each excitation is affected by the previous pulses by means of Stark shift. Therefore, the amount of this Stark shift is proportional to the temporal integration of the laser intensity, before the pulse arrives, and it is again proportional to the averaged laser intensity. It is noteworthy, however, that in the strong-field regime experiments, the Stark shift depends on the pulse peak power [20] (enough to induce Z rotations in sub-picosecond time scales).

4. Conclusion

In summary, we performed DFCS of ^{133}Cs $6s^2S_{1/2}$–$8s^2S_{1/2}$ two-photon transitions. We utilized the counter-propagating beam geometry of spectrally encoded ultrafast laser pulses to probe the two-photon transitions of atomic cesium. When being compared with theory and previous measurements, our measured Doppler-free transition profiles are in a good agreement. The absolute frequencies of these transitions are determined with uncertainty below 5×10^{-10} and our error analysis concludes that the main cause of uncertainty comes from laser-induced AC Stark shift.

Acknowledgments

This research was supported by Samsung Science and Technology Foundation [SSTF-BA1301-12].

ORCID iDs

Jaewook Ahn https://orcid.org/0000-0002-5837-6372

References

[1] Udem T F, Holzwarth R and Hänsch T W 2002 Optical frequency metrology *Nature* **416** 233
[2] Baklanov Y F and Chebotayev V P 1977 Narrow resonances of two-photon absorption of super-narrow pulses in a gas *Appl. Phys.* **12** 97
[3] Parthey C G *et al* 2011 Precision measurement of the hydrogen 1*S*-2*S* frequency via a 920-km fiber link *Phys. Rev. Lett.* **107** 203001
[4] Mohr P J, Taylor B N and Newell D B 2008 CODATA recommended values of the fundamental physical constants: 2006 *Rev. Mod. Phys.* **80** 633
[5] Fischer M *et al* 2004 New limits on the drift of fundamental constants from laboratory measurements *Phys. Rev. Lett.* **92** 230802
[6] Dickenson G D, Niu M L, Salumbides E J, Komasa J, Eikema K S E, Pachucki K and Ubachs W 2013 Fundamental vibration of molecular hydrogen *Phys. Rev. Lett.* **110** 193601
[7] Meyer V *et al* 2000 Measurement of the 1*S*-2*S* energy interval in muonium *Phys. Rev. Lett.* **84** 1136
[8] Rosenband T *et al* 2008 Frequency ratio of Al^+ and Hg^+ single-ion optical clocks; metrology at the XVII decimal place *Science* **319** 1808
[9] Coddington I, Swann W C, Nenadovic L and Newbury N R 2009 Rapid and precise absolute distance measurements at long range *Nat. Photonics* **3** 351
[10] Barmes I, Witte S and Eikema K S E 2013 Spatial and spectral coherent control with frequency combs *Nat. Photonics* **7** 38
[11] Barmes I, Witte S and Eikema K S E 2013 High-precision spectroscopy with counterpropagating femtosecond pulses *Phys. Rev. Lett.* **111** 023007
[12] Marian A, Stowe M C, Lawall J R, Felinto D and Ye J 2004 United time-frequency spectroscopy for dynamics and global structure *Science* **306** 5704
[13] Fendel P, Bergeson S D, Udem T and Hänsch T W 2007 Two-photon frequency comb spectroscopy of the 6*s*-8*s* transition of cesium *Opt. Lett.* **32** 701
[14] Jones D J, Diddams S A, Ranka J K, Stentz A, Windeler R S, Hall J L and Cundiff S T 2000 Carrier-envelope phase control of femtosecond mode-locked lasers and direct optical frequency synthesis *Science* **288** 635
[15] Lee W, Kim H, Kim K and Ahn J 2015 Coherent control of resonant two-photon transitions by counter-propagating ultrashort pulse pairs *Phys. Rev.* A **92** 033415
[16] Stalnaker J E, Mbele V, Gerginov V, Fortier T M, Diddams S A, Hollberg L and Tanner C E 2010 Femtosecond frequency comb measurement of absolute frequencies and hyperfine coupling constants in cesium vapor *Phys. Rev.* A **81** 043840
[17] Hagel G, Nesi C, Jozefowski L, Schwob C, Nez F and Biraben F 1999 Accurate measurement of the frequency of the 6*S*-8*S* two-photon transitions in cesium *Opt. Commun.* **160** 1
[18] Demtröder W 2008 *Laser Spectroscopy* vol. 1 (Heidelberg: Springer)
[19] Felinto D, Acioli L H and Vianna S S 2000 Temporal coherent control of a sequential transition in rubidium atoms *Opt. Lett.* **25** 917
[20] Lim J, Lee H, Lee S, Park C-Y and Ahn J 2014 Ultrafast Ramsey interferometry to implement cold atomic qubit gates *Sci. Rep.* **4** 5867
[21] Steck D A Cesium D line data http://steck.us/alkalidata/cesiumnumbers.pdf